Research on Engineering Structures & Materials
www.jresm.org

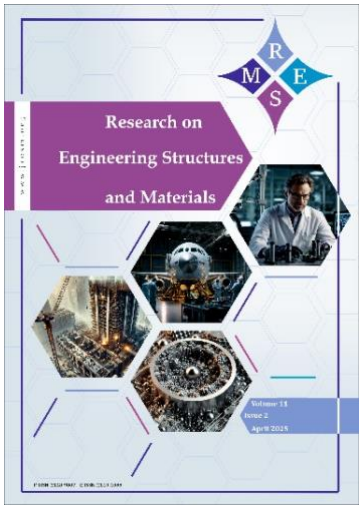

Synergetic use of ground granulated blast furnace slag and sugarcane bagasse ash to develop green concrete

Neeraja P.G., Sujatha Unnikrishnanan, Alwyn Varghese

Online Publication Date: 30 January 2026

URL: http://www.jresm.org/archive/resm2026-1036ma0723rs.html
DOI: http://dx.doi.org/10.17515/resm2026-1036ma0723rs

Journal Abbreviation: *Res. Eng. Struct. Mater.*

To cite this article
Neeraja P G , Unnikrishnanan S, Varghese A. Synergetic use of ground granulated blast furnace slag and sugarcane bagasse ash to develop green concrete. *Res. Eng. Struct. Mater.*, 2026; 12(3): 1831-1849.

Research on Engineering Structures & Materials
www.jresm.org
Research Group

Research Article

Synergetic use of ground granulated blast furnace slag and sugarcane bagasse ash to develop green concrete

Neeraja P.G. [*,1,2,a], Sujatha Unnikrishnanan [1,b], Alwyn Varghese [2,c]

[1]*Department of Civil Engineering, Christ University, Bengaluru, India*
[2]*Department of Civil Engineering, Jyothi Engineering College, Kerala, India*

Article Info

Article History:

Received 23 July 2025

Accepted 25 Jan 2026

Keywords:

Sustainable construction;
GGBS-SCBA concrete;
Mechanical properties;
Microstructural analysis,
SEM-XRD techniques

Abstract

Considering the need for sustainable materials, this research involves mechanical and microstructure studies of concrete including ground granulated blast furnace slag (GGBS) and sugarcane bagasse ash (SCBA). Ordinary Portland cement (OPC) was partially replaced by GGBS and SCBA and M sand was substituted in part by SCBA. The experimental studies included tests for compressive strength, tensile strength and flexural strength, along with microstructural analysis through Scanning Electron Microscopy (SEM) and Energy-Dispersive X-ray Spectroscopy (EDX). The results shows that GGBS improves the workability of concrete, whereas SCBA tends to reduce it. In combination, these materials exhibit a complementary directing to a denser microstructure. The Strength of concrete with 35% replacement of OPC is comparable to that of the reference concrete. Based on test results an empirical relation was developed for the compressive and flexural strengths. The optimum mixes with 20-35 % binder replacement gives a carbon di oxide saving of 95-110 kg CO2/m3. Overall, the study summarizes that incorporating these materials supports the production of environmentally responsible concrete.

1. Introduction

The construction industry is now focusing more on sustainability. In that situation industry is demanding more on the development of green concrete by utilising agro-industrial wastes. Commonly used industrial by products are Fly ash, Silica fume, Ground Granulated Blast-Furnace Slag (GGBS) and Sugarcane Bagasse Ash (SCBA), etc. Similarly, natural river sand over-consumption is also a major concern. There are many alternative materials available for sand replacement also. This study focused on replacing part of Ordinary Portland Cement (OPC) with GGBS and SCBA. SCBA is also incorporated as a partial substitute for fine aggregate. The aim of this study is to see how these materials can contribute to strength development and reduction in carbon dioxide emission.

India produces a large amount of bagasse ash from sugarcane, almost 100 million tonnes every year [1, 2]. Many types of ash that contains an adequate quantity of silica and alumina comparable to cement, are not used effectively. These ashes cause various types of environmental issues [3]. Steel plants in India also produce GGBS as a by-product, with some making over 3.78 million tonnes per year [4]. Using GGBS in concrete helps recycle industrial waste and lowers the carbon footprint of cement production. Research shows that SCBA reacts well with cement, helping concrete gain strength faster and last longer [1]. Using up to 5% SCBA as a cement replacement can improve strength and durability. Sugarcane Bagasse ash can replace a small portion of fine aggregate without reducing compressive strength [2, 5].

*Corresponding author: pgneeraja@gmail.com
[a]orcid.org/0009-0006-9831-5749; [b]orcid.org/0000-0001-6444-4258 ; [c]orcid.org/0000-0002-4916-6293
DOI: http://dx.doi.org/10.17515/resm2026-1036ma0723rs

Prior research has examined the application of SCBA as a partial sand replacement in mortar for pavement crack repair. Those studies mainly focussing on analysing its influence on compressive strength, shrinkage, and tensile behaviour [6,7]. Some other studies have shown that combining SCBA with silica fume as a partial cement substitute in mortar enhances both compressive and flexural strength [8]. A summary of previous studies related to the replacement of cement with GGBS or SCBA is presented in Table 1. The overall findings from these studies reveals the environmental advantages of using GGBS and SCBA as partial replacement to Ordinary Portland Cement (OPC).

Table 1. Summary of research trends based on the literature survey

Reference	Constituent material	% Replacement	Workability Trend	Compressive Strength (fck)	Split Tensile Strength (fct)
Chusilp et al. [9]	SCBA	0–30%	Limited data reported	20% replacement showed ~13% increase	Not reported
Bahurudeen & Santhanam [10]	SCBA	0–30% (processed ash)	Depends on processing condition	Pozzolanic efficiency improved strength	Not reported
Ramakrishnan et al.[11]	SCBA as Fine Aggregate	0–30%	Acceptable workability	Optimum strength at 10% replacement	Improved compared to control
Arenas-Piedrahita et al. [12]	SCBA + Fly Ash	0–30%	Moderate effect on fresh properties	Slight decrease observed in untreated ash mixes	Decline due to weak bonding
Kumar et al. [13]	GGBS	0–40%	Slight improvement in flow	Higher strength at optimum replacement	Improved splitting strength
Phul et al. [14]	GGBS + Fly Ash	0–40%	Improved workability	Increased compressive strength	Not reported
Khalil et al. [15]	SCBA (review work)	Up to 30–40%	Depends on treatment & fineness	Reported strength gains with optimized ash	Some studies show improvement
Wu et al. [16]	SCBA (UHPC)	0–30%	High reactivity, acceptable workability	Increased compressive strength in UHPC	Not applicable / not reported
Liu et al. [17[	Fly Ash / GGBS	0–60%	Better flowability	Higher long-term strength	Not reported
Venkat et al. [18]	Silica fume, Metakaolin, GGBS	0–20%	Better fresh performance	Higher early and final strength	Better splitting value
Krishna et al. [19]	GGBS	0–50%	Negligible effect	Good strength under optimal curing	Enhanced tensile values
Abdalla et al. [20]	Silica Fume + High SCBA	0–40%	Slight reduction in flow	Good improvement in blended mixes	Not reported
Sobuz et al. [21]	SCBA	0–30%	Acceptable flowability	Enhancement supported by ML prediction	Not explicitly reported

The present study seeks to assess the impact of GGBS and SCBA on the mechanical strength of concrete when used as binder materials, along with assessing the effect of partially substituting fine aggregate with SCBA. These mechanical properties such as compressive strength tensile strength and flexural strength serve as key indicators of a concrete's structural reliability and expected service life [22]. Microstructural evaluation using Scanning Electron Microscopy (SEM), X-Ray Diffraction (XRD), and Energy-Dispersive X-ray (EDX) analysis to better understand the morphology. Through these investigations, the work aims to provide a detailed perspective on how

the combined use of GGBS and SCBA can contribute to producing durable, sustainable concrete without sacrificing strength or overall performance

2. Materials and Methods

2.1 Materials

Concrete specimens in the present investigation were prepared using Ground Granulated Blast Furnace Slag (GGBS) and Sugarcane Bagasse Ash (SCBA) as key constituents for the development of blended cement. The SCBA was obtained from KPR Sugar Mill, Coimbatore, India. Ordinary Portland Cement conforming to IS 8112:2013, manufactured sand (M-sand), coarse aggregates with a maximum size of 20 mm, and water were used for casting. In this study, SCBA was utilized in two ways: as a binder replacement and as a fine aggregate replacement. The collected SCBA was sieved through a 90 µm sieve and the particles passing the sieve were used for cement replacement. Table 2 gives the details of the comparison of the chemical composition of OPC, GGBS, and SCBA and the physical properties are shown in Table 3.

Table 2. Chemical composition of OPC, GGBS, and SCBA

Constituents	OPC (% by mass)	GGBS (% by mass)	SCBA (% by mass)
Magnesia (MgO)	06.45	006.45	01.21
Lime (CaO)	64.64	38.69	08.55
Silica (SiO2)	21.28	32.60	62.11
Alumina (Al2O3)	05.60	17.88	03.55
Ferric Oxide (Fe2O3)	03.36	02.19	01.55
Chloride (Cl)	00.10	0.009	0.010
Loss on Ignition	00.64	00.00	20.44

Table 3. Physical characteristics of OPC, GGBS and SCBA

Sl. No.	Test	OPC	GGBS	SCBA
1	Fineness	3.25%	7.2%	5.6%
2	Standard Consistency	36%	35%	35%
3	Specific gravity	3.19	2.9	2.22
4	Initial setting time	40 min.	70 min.	80 min.

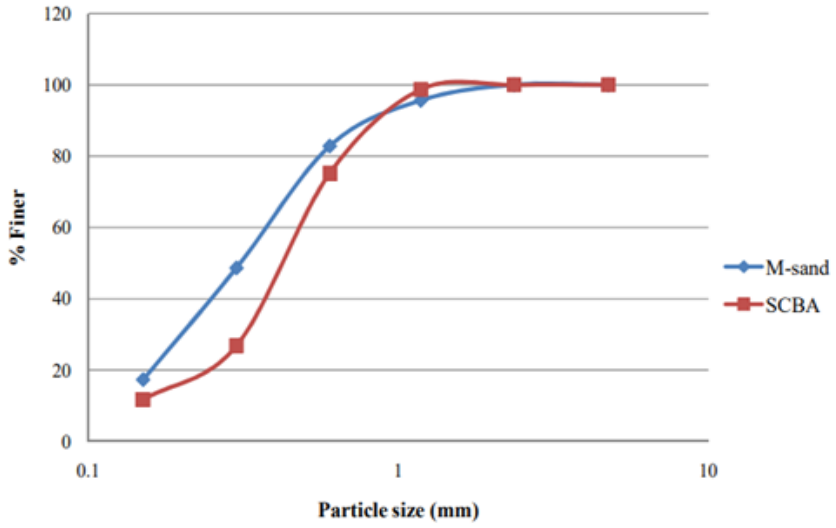

Fig. 1. Particle size distribution curve for M-sand and SCBA

Fig. 1 shows the PSD of M sand and SCBA used for the partial replacement of fine aggregate. Well-graded fine aggregates ensure proper packing, reduced voids, and improved density, which directly influence the strength and durability of concrete. From the PSD curve, it is evident that M-sand

shows a more continuous grading pattern, while SCBA has a finer particle fraction that approaches the grading limits of fine aggregates specified in standards such as IS 383:2016. SCBA can be incorporated either as a fractional substitution of fine aggregate or as a fine filler blended with M-sand. The PSD curve highlights that SCBA has a slightly coarser fraction compared to M-sand at smaller particle sizes but attains near-similar fineness at higher passing percentages.

2.2 Concrete Mixing and Casting

Table 4 illustrates the different mix proportions in which cement was partially replaced with GGBS and SCBA. Fine aggregate is also partially replaced with SCBA in a few mixes. Slump values showed noticeable changes with the inclusion of SCBA and GGBS to the mix. According to the mix design for 1 m^3 of concrete, the material requirements are as follows: 410 kg of cement (OPC 53 grade), 630 kg of fine aggregate, and 1182 kg of coarse aggregate, with a water–binder of 0.47, targeting M25 grade concrete, without the addition of superplasticizer.

Table 4. Composition of constituent materials of concrete in percentage

Mix Id	Binder Composition (% By Mass)			FA (% By Mass)	
	GGBS	SCBA	OPC	SCBA	M Sand
A01	0	0	100	0	100
A11	10	10	90	0	100
A12	20	10	80	0	100
A13	30	10	70	0	100
A14	40	10	60	0	100
A21	10	10	80	5	95
A22	20	10	70	5	95
A23	30	10	60	5	95
A24	40	10	50	5	95
A31	10	15	75	0	100
A32	20	15	65	0	100
A33	30	15	55	0	100
A34	40	15	45	0	100
A41	10	15	85	5	95
A42	20	15	75	5	95
A43	30	15	65	5	95
A44	40	15	55	5	95
A51	10	15	80	10	90
A52	20	15	70	10	90
A53	30	15	60	10	90
A54	40	15	50	10	90

Fig. 2. Concrete samples prepared for strength testing

Concrete workability was determined by slump cone test. Following the procedure outlined in IS 1199:2018 [23]. The concrete specimen for testing is shown in Fig 2. Compressive strength, split tensile, and flexure strength of concrete were examined as per IS516:2021(section 1 part 1) [24]. Concrete cubes of size 150mmx150mmx150mm were tested for compressive strength after 7 days, 28 days, 56 days, and 90 days of curing. Whereas cylinders of 150 mm diameter and 300mm height were tested after 28 days of curing for split tensile strength. Flexural strength was determined by testing beams of size 100mm x 100mm x 500mm after 28days of curing. A total of five samples were prepared and tested for each mix proportion. In addition, the microstructure of the developed concrete was studied using a scanning electron microscope (SEM) and X-ray diffraction (XRD).

2.3 Methodology

This study is organized as shown in Fig.3. The mechanical strength tests were conducted in compliance with IS 516:2021 using a load-controlled Universal Testing Machine (UTM) with a capacity of 2000 kN. All specimens were maintained in water-curing tank at a temperature of 28–30°C, and tested as illustrated in Fig. 4. The load was gradually applied at a constant rate without any sudden impact up to the point of failure, and the resulting collapse load was documented. Concrete cubes were tested at 7, 28, 56, and 90 days of curing and the compressive strength was determined using the equation fc = P/A, where P = maximum load at failure (N), and A = loaded area of specimen (mm^2).

For Split Tensile Strength Cylindrical specimens were tested in accordance with IS 516:2021. Thin plywood strips were positioned at the top and bottom of each specimen to ensure uniform load distribution. The split tensile strength was calculated using:

$$fst = \frac{2P}{\pi LD} \tag{1}$$

where P = maximum load at failure (N), L = length of cylinder (mm), and D = diameter of cylinder (mm).

For Flexural Strength beams were tested using the three-point bending method (central loading) in accordance with IS 516: 2021.The modulus of rupture was calculated using:

$$fr = \frac{3PL}{2BD} \tag{2}$$

where P = maximum load at failure (N), L = span length (mm), B= specimen width (mm), and D= specimen depth (mm).

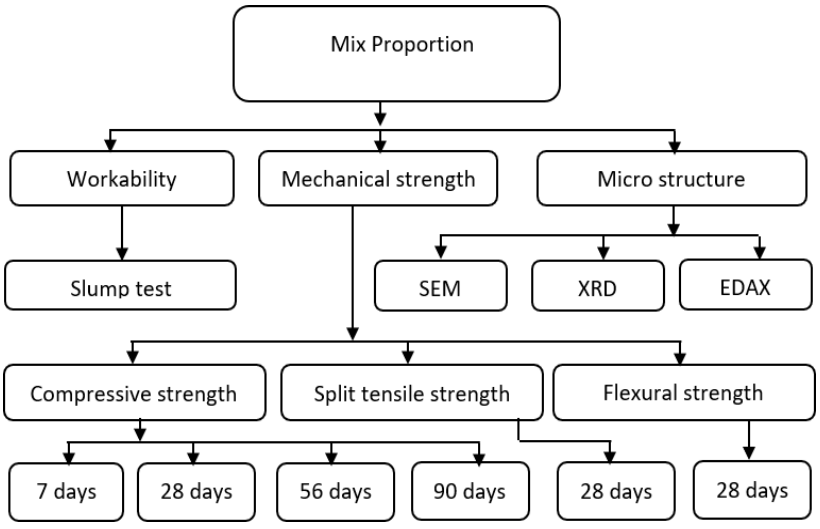

Fig. 3. Overview of the experimental investigation

Fig. 4. Experimental setup for Mechanical strength testing

3. Results and Discussion

3.1 Fresh Properties

As per IS1199: 2028 workability of concrete was assessed by slump cone test. Slump values were varied between 75mm to 120 mm. It is noted that higher the GGBS percentage there is an increase in slump values. GGBS has a fine and smooth texture which improves fluidity and aids air entrainment within the mix. In contrast it is found that slump values declined when percentage of SCBA is more. This can be attributed to the high porosity and large specific surface area of SCBA, resulting in increased water absorption and altered moisture distribution [26,27].

3.2 Compressive Strength

Incorporating GGBS and SCBA as fractional substitutes for the binder and fine aggregate resulted in comparable strength performance across different concrete grades. Fig. 5 shows the compressive strength at 7, 28, 56, and 90 days. The mix containing 30% binder replacement and 5% fine aggregate replacement gained a 28-day strength of 31.6 MPa, while mixes with 35–40% binder replacement and 0–5% fine aggregate replacement attained strengths between 27 and 28.5 MPa [25].

Several blended mixes also exhibited higher early-age strength than the control (15.5 MPa). After 7 days, mixes A12, A21, A31, A43, and A52 developed strengths of 17.21, 21.46, 22.48, 18.08, and 16.13 MPa, respectively showing improvements of 11.0%, 38.5%, 45.1%, 16.6%, and 4.1%. This improvement may be attributed to reactive silica in SCBA and the accelerated hydration promoted by GGBS [25,28]. By 56 days, the mixes reached 32.43–33.73 MPa, corresponding to a 0.6–4.6% increase over the control (32.24 MPa) [29]. At 90 days, strengths ranged from 34.35 to 36.67 MPa. Mix A12 showed a slight reduction (−3.7%). But A22 and A32 recorded gains of +0.3% and +2.8%, respectively [29].

From these results it indicates that replacing up to 30–35% of the binder using a combination of GGBS and SCBA can achieve compressive strengths similar to conventional OPC concrete. Improvements in in strength at 90 days was more pronounced at SCBA levels above 10%, whereas fine aggregate replacement had minimal influence. These findings confirm the effective use of these supplementary cementitious materials for sustained strength development [30].

3.3 Split Tensile Strength

The split tensile strength evaluation at 28 days was as per IS 516:2021, as displayed in Fig. 6, exhibits a parallel pattern to that observed in compressive strength. The binary blends yielded inferior strength outcomes compared to the control. Prior research on split tensile strength confirms these findings for higher-volume replacements. Researchers observed a decline in strength below that of the control concrete when the replacement of SCBA exceeded 20% [31, 32, 33].

The concrete mix with 20% GGBS and 10% SCBA along with cement and binder has shown maximum split tensile strength which is very close to that of reference mix (3% less than control mix). The concrete mix with 20% GGBS and 10% SCBA as binder replacement along with 5% SCBA as fine aggregate replacement exhibited a split tensile strength of 4.33 MPa, which is about 8.8% less than the control mix, indicating a minor reduction in tensile strength. The concrete mix with 20% GGBS and 15% SCBA as binder replacement achieved a split tensile strength of 4.32 MPa, showing a 9.1% reduction in comparison with the reference mix, suggesting that higher SCBA content slightly lowers tensile strength.

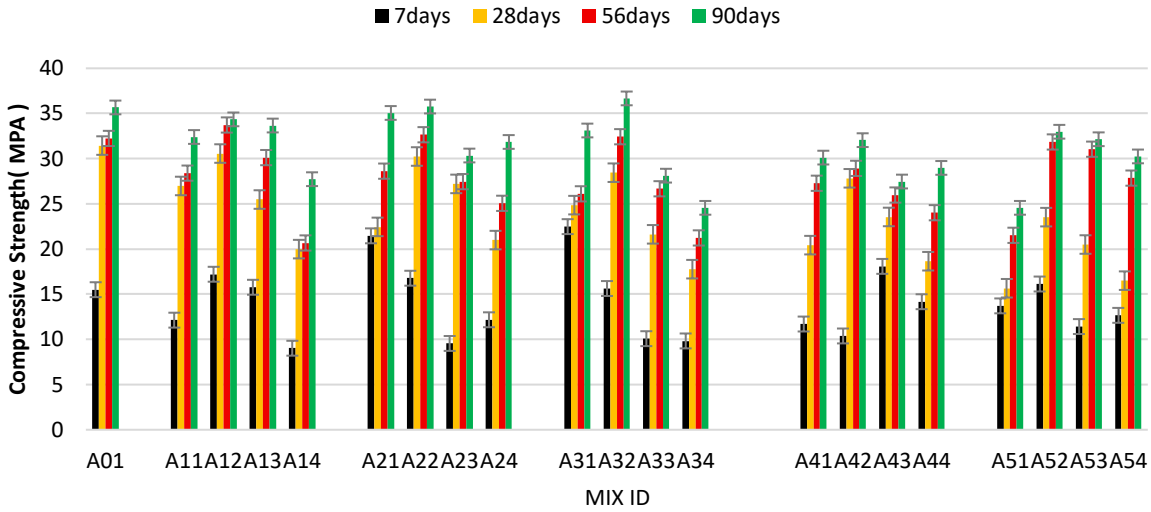

Fig. 5. Compressive strength

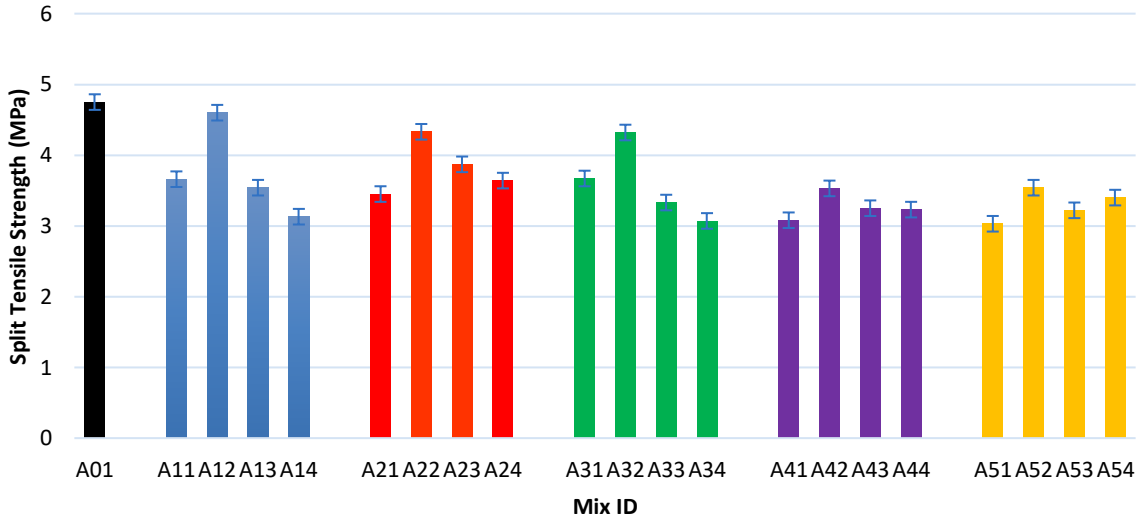

Fig .6 . Split tensile strength

3.4 Flexural Strength

Fig. 7 illustrates the flexural strength of concrete beams (100 mm × 100 mm × 500 mm) incorporating different proportions of SCBA and GGBS, tested after 28 days of curing. The graph shows that flexural strength increases with GGBS replacement up to 20%. It is evident that when the GGBS replacement level is on higher side there observed a reduction in flexural strength [34, 35]. Mixes A12, A22, A32, and A42 achieved values comparable to the control mix (A01, 3.95 MPa), conversely mixes with higher binder and fine aggregate replacement, such as A14, A34, and A54,

showed lower strength. The trend depicted in the graph emphasizes that excessive use of supplementary materials can negatively affect the concrete's flexural behavior.

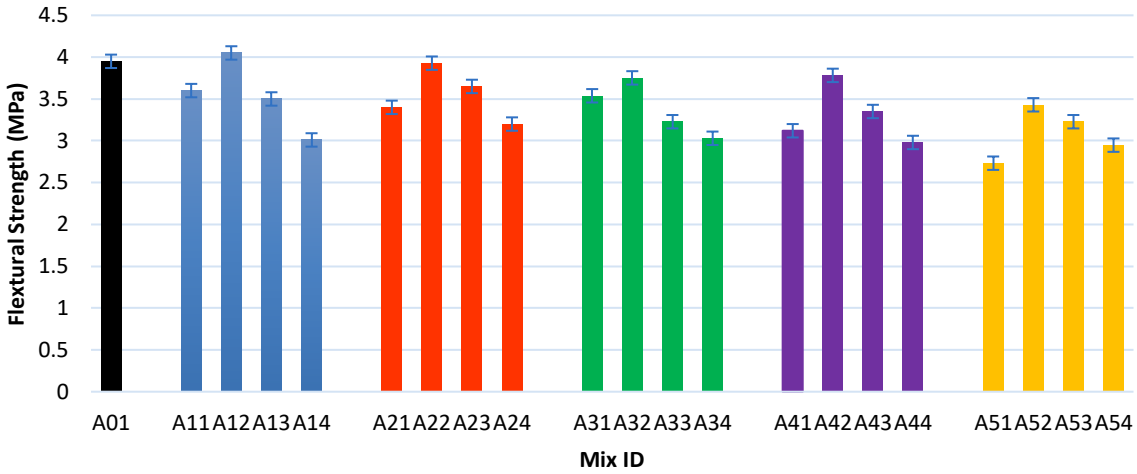

Fig. 7. Flexural strength

2.5 Development of Empirical Relationship

An Empirical model was formulated to establish the connection between compressive strength and GGBS replacement levels ranging from 0 to 40%. The average compressive strengths corresponding to 0-40% replacement was 31.45, 25.45, 26.78, 28.97, and 22.67 MPa, respectively.

In this series, the only substance used to substitute cement was GGBS. Five test concrete cubes were used to assess each substitution level, and the mean data were used to create the model in order ensure reliability and accuracy. Equation 1 was developed according to the test result, and the R^2 value is obtained as 0.886.

$$fck\ GGBS\ (Y) = -1.3\ x10^{-3}(\%\ of\ GGBS)^3 + 0.0782(\%\ of\ GGBS)^2 - 1.2658(\%\ of\ GGBS) + 31.469 \quad (3)$$

The compressive strength with varying percentages of GGBS 0- 40 % is shown in Fig. 8. Five trials (T1-T5) were conducted for each replacement level. The average compressive strength values (AV) from these trials were plotted against the corresponding GGBS replacement percentages. A polynomial trend line was fitted to the average data points to represent the relationship between compressive strength and GGBS content.

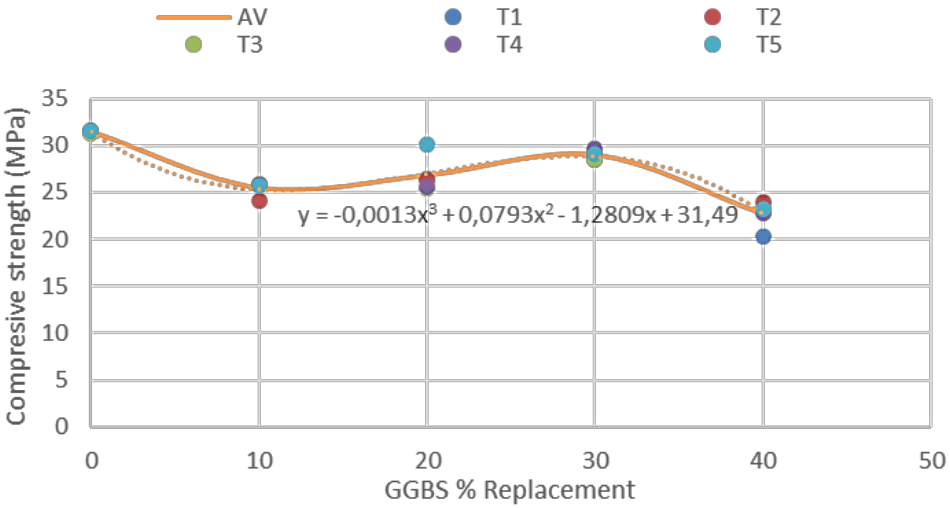

Fig. 8. Compressive strength of concrete with GGBS replacement levels

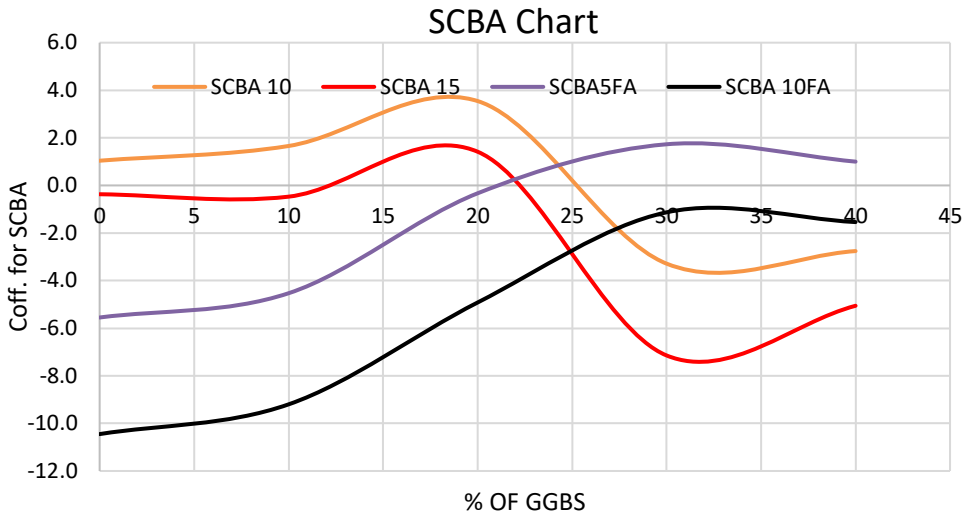

Fig. 9. Coefficient of SCBA

The influence of SCBA was analysed separately in Fig.9 and added as a correction coefficient to the model. Equation 2, which expresses the final compressive strength of concrete, can be accurately predicted by combining Equation 1 and SCBA coefficient. For concrete mixtures with different ratios of GGBS and SCBA, the validation results shown in Fig.10 demonstrate that the percentage error is less than 5%, validating the resilience and dependability of the suggested model.

$$Fck = fck\ GGBS\ + Coefficient\ of\ SCBA\ + Coefficient\ of\ SCBA\ FA \tag{4}$$

The flexural strength equation was developed by adding a polynomial term, expressed in terms of GGBS percentage along with the standard relation $0.7\sqrt{Fck}$. By combining this term with the standard relation, the final flexural strength prediction model was formulated as Equation 3 for which the R^2 value was obtained as 0.875. This model accurately captures the effect of GGBS and SCBA replacement on flexural strength. Validation confirmed that this model provides improved accuracy compared to the standard relation and is shown in Fig.11.

$$Ft = 0.7\sqrt{Fck} + 0.0006(\%\ of\ GGBS)^2 + 0.0226(\%\ of\ GGBS) - .1147 \tag{5}$$

where Ft is the flexural strength of concrete with compressive strength Fck from Equation 4.

Table 5. Performance metrics for compressive strength

Dataset	RMSE	MAE	MAPE (%)	R^2
Training	0.322	0.266	1.13	0.9955
Test	0.236	0.168	0.71	0.9975

Table 6. Performance metrics for flexural strength

Dataset	RMSE	MAE	MAPE (%)	R^2
Training data	0.164	0.116	3.47	0.803
Test data	0.104	0.077	2.30	0.918

Table 5 displays the performance metrics of the developed predictive model for compressive strength during the training and testing phases. The model exhibits excellent accuracy and reliability in both datasets. For the training dataset, the Root Mean Square Error (RMSE) and Mean Absolute Error (MAE) are 0.322 and 0.266, respectively, shows low prediction errors. The Mean Absolute Percentage Error (MAPE) of 1.13% confirms the high precision of the model. An R^2 value of 0.995 indicates strong correlation between experimental and predicted compressive strength values. The Lower RMSE, MAE, and MAPE values for test further more improves the modal performance. In summary the low errors values and high R^2 for both training and testing confirms that the proposed model is effective for forecasting compressive strength.

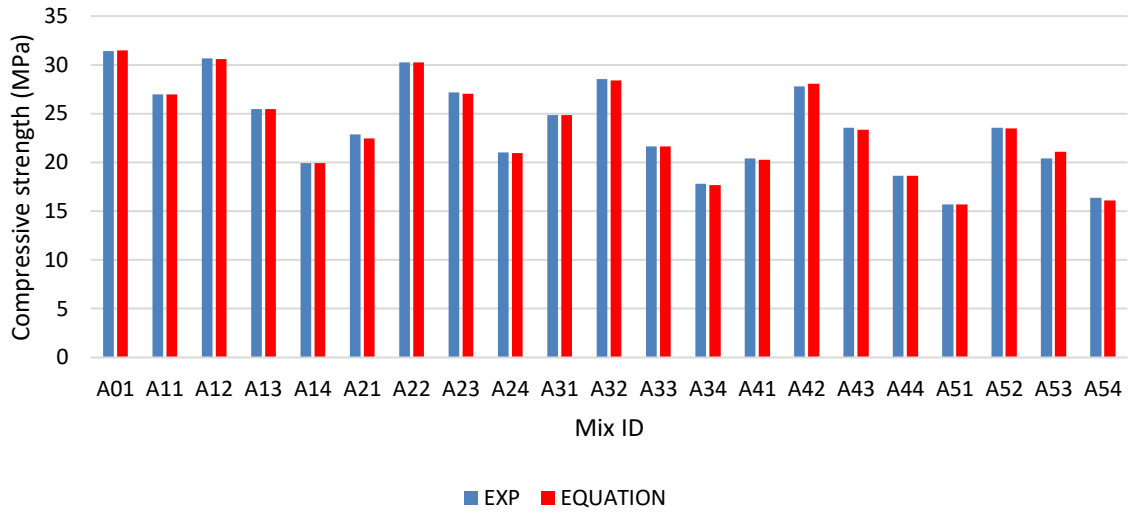

Fig. 10. Comparison of experimental and predicted 28-day compressive strength

Fig. 11. Comparison of experimental and predicted split tensile strength

Table 6 summarize the RMSE, MAE, MAPE and R2 values for flexural strength prediction using both training and testing data set. The training dataset attained RMSE and MAE values of 0.164 and 0.116 with MAPE of 3.47 % and R2 of 0. 803.It shows good learning capacity of the mode. For the test dataset lower RMSE, MAE and MAPE and higher R2 value showed a strong agreement between predicted and experimental results. However, the model has limitations. The test data set is small, which may make the validation results less representative. Also, the model was trained only on experimental data from controlled lab conditions its applicability is confined to similar material compositions, mix proportions, and curing conditions. Therefore, and caution should be exercised when extrapolating the results to other conditions.

3.6 Morphology of GGBS and SCBA

The scanning electron microscopy (SEM) analysis of GGBS and SCBA, presented in Fig. 12. It highlights their distinct morphological characteristics. SCBA particles exhibit a fibrous, irregular shape with a porous structure, whereas GGBS particles display an angular, irregular surface texture. The porosity in SCBA is largely attributed to residual unburned carbon.

Elemental analysis using Energy-Dispersive X-ray Spectroscopy (EDX), shown in Fig.13, indicates that GGBS contains silica, calcium, aluminium, and other trace elements, while SCBA is predominantly composed of silica. Chemical oxide compositions of GGBS and SCBA were

ascertained through XRF analysis as shown in Table 2. GGBS is characterized by significant proportions of calcium oxide, silicon dioxide, and aluminum oxide, constituting 38.69%, 32.6%, and 17.88%, respectively, with calcium oxide dominating.

On the other hand, SCBA predominantly comprises silicon dioxide, accounting for 62.11% of its chemical composition. The study underscores the high calcium oxide content in GGBS, which leads its crucial role in the overall composition, while SCBA stands out for its silicon dioxide-rich nature. The Ca/Si ratio of OPC, GGBS & SCBA are 3.037, 1.186 and 0.137 respectively.

XRF analysis of SCBA shows about 62.11% SiO_2, 3.55% Al_2O_3, 1.55% Fe2O3, and 8.55% CaO. Furthermore, LOI of SCBA is 20.74%. Previous studies have identified that the elevated LOI observed in SCBA is primarily owing to the high carbon levels in unburned fibrous particles [36]. These residual carbon-rich fibers result from incomplete combustion during the bagasse burning process, leading to increased LOI values in the ash. This high LOI can adversely affect the pozzolanic activity of SCBA, thereby limiting its effectiveness as a alternative cementitious material in concrete applications. Presence of partially and unburned fibrous particles in SCBA was noticed by other researchers [37]. This thorough analysis provides a foundation for examining the mutual effects of GGBS and SCBA on the characteristics and performance of blended cements, yielding important insights for sustainable construction materials.

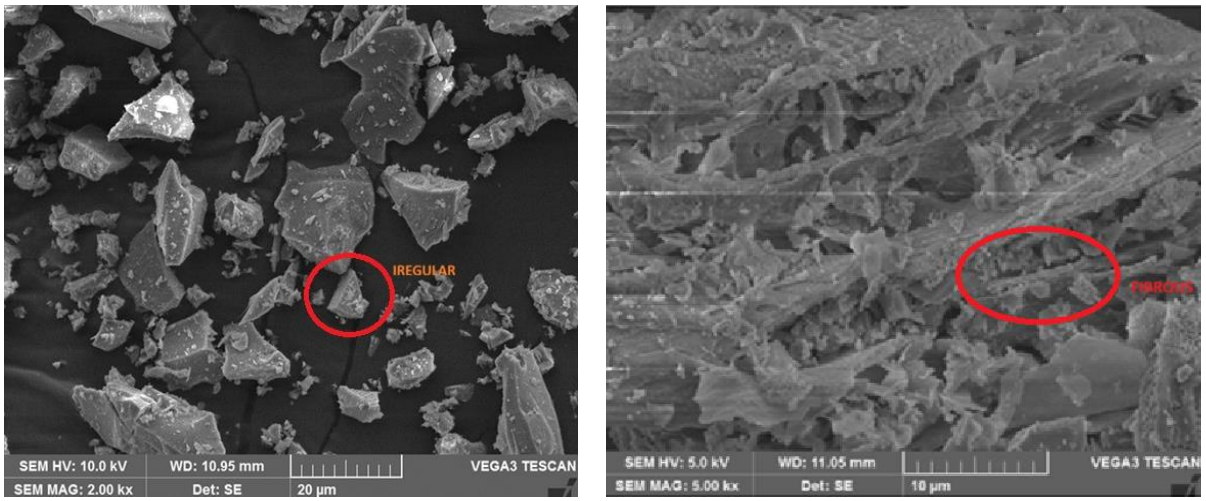

Fig. 12. SEM micrograph showing the morphology of GGBS and SCBA particles

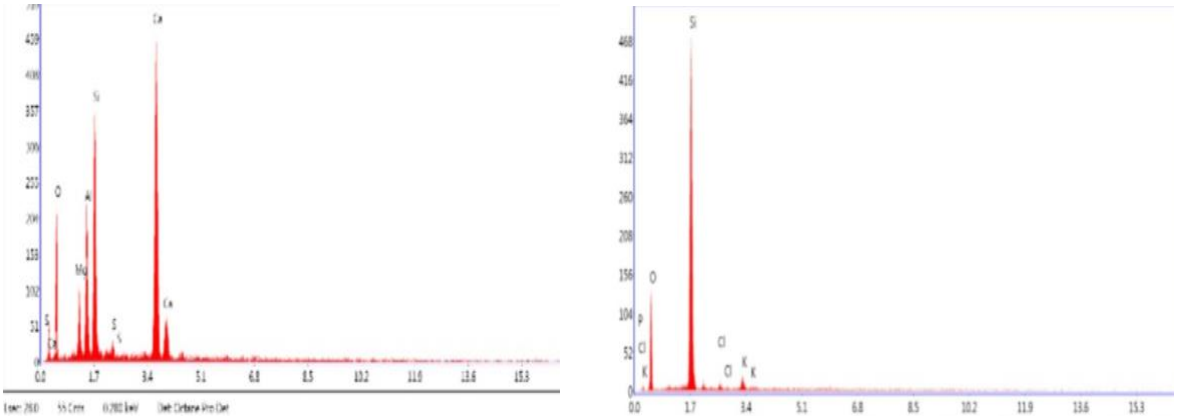

(a) (b)

Fig. 13. EDX images of (a) GGBS and (b)SCBA

The XRD of GGBS and SCBA are presented in Fig. 14 and Fig. 15 respectively. The XRD pattern of GGBS indicates a semi-crystalline structure, with the majority of the material existing in an amorphous phase with peak at 2 theta values of 28 degree. In contrast, the XRD pattern of SCBA reveals multiple crystalline phases, with dominant peaks corresponding to Quartz (crystalline SiO_2)

in a hexagonal structure, marked as Q which is observed at 2 theta value of 29.443-degree Additional peaks are observed for Al_2O_3 (Corundum) with a rhombohedral crystal structure, marked as C, and for Fe_2O_3 with a cubic crystal structure, marked as H.

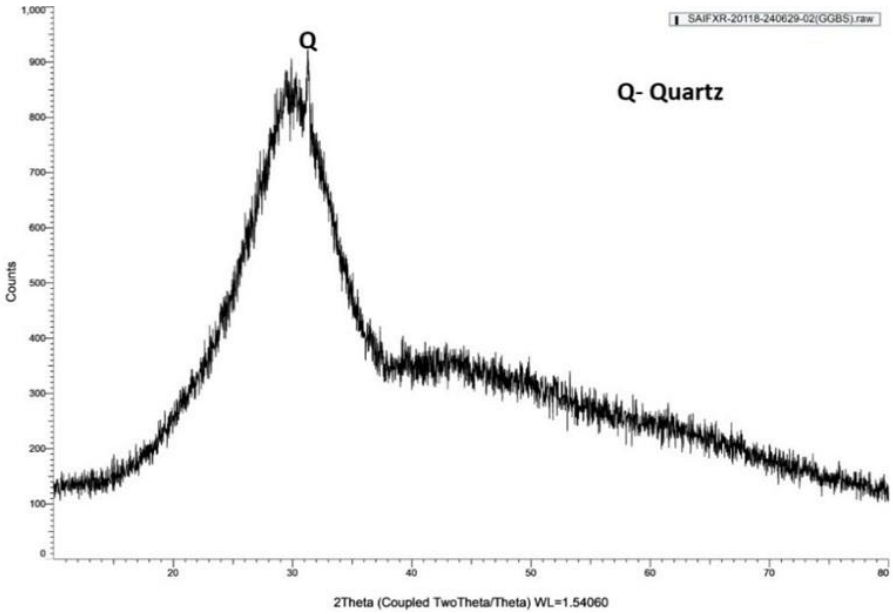

Fig.14. XRD image of GGBS

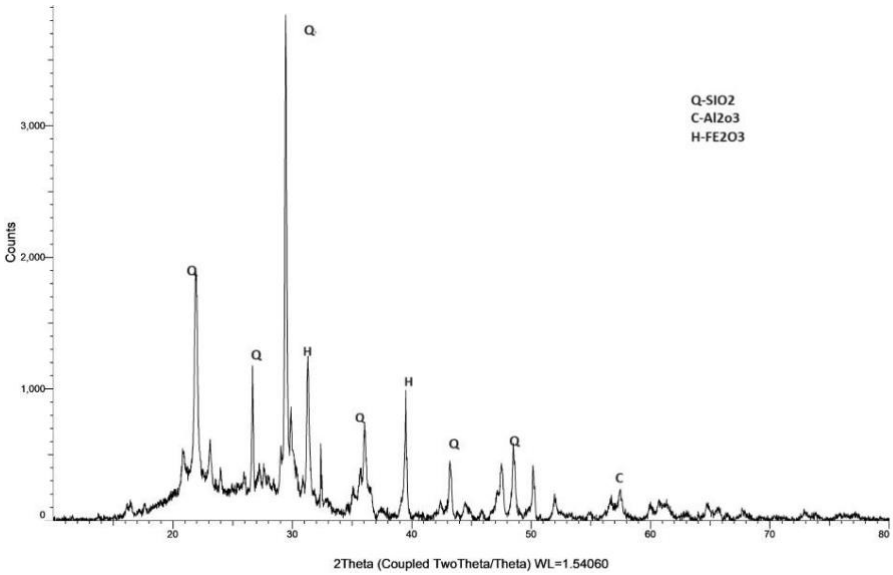

Fig. 15. XRD image of SCBA

3.7 Microstructure Analysis of Binary Mixes

SEM was performed using a TESCAN VEGA3 machine with a resolution of at least 10 nm. SEM images were taken from 28-day-old concrete specimens. EDX was most likely done concurrently with SEM. EDX is used to determine the elemental breakdown of materials. In the case of concrete, EDX would provide information about the chemical composition of the phases observed [38]. This helps to understand how elements and phases are distributed throughout the concrete microstructure [39]. Mix with higher strength in each category was selected for microstructure analysis using SEM and possibly EDX, providing insights into their microstructural characteristics and potential performance differences.

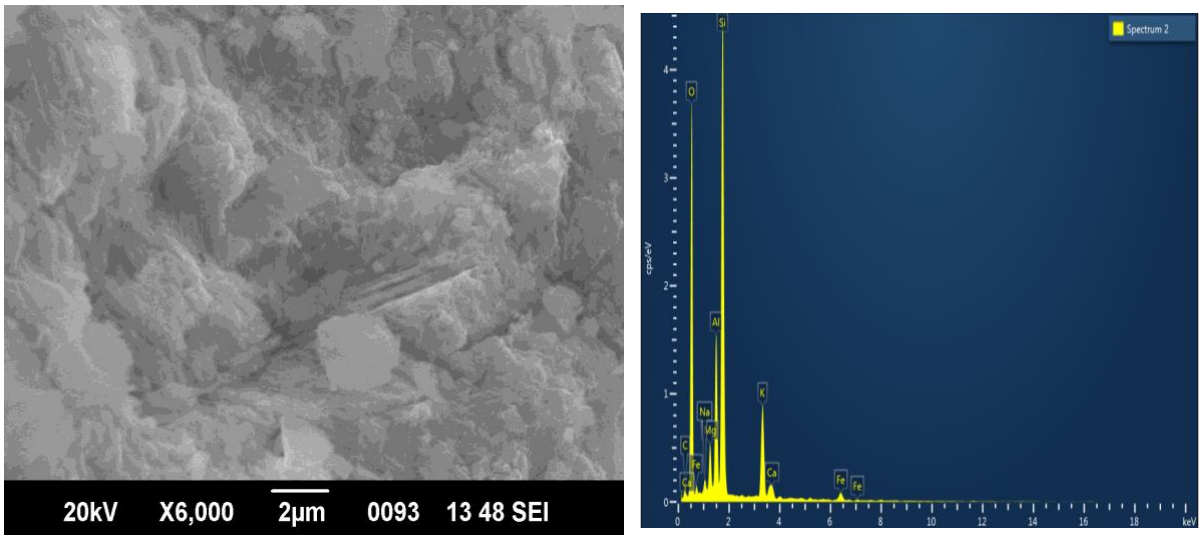

Fig. 16. SEM micrograph and EDX analysis of the control concrete

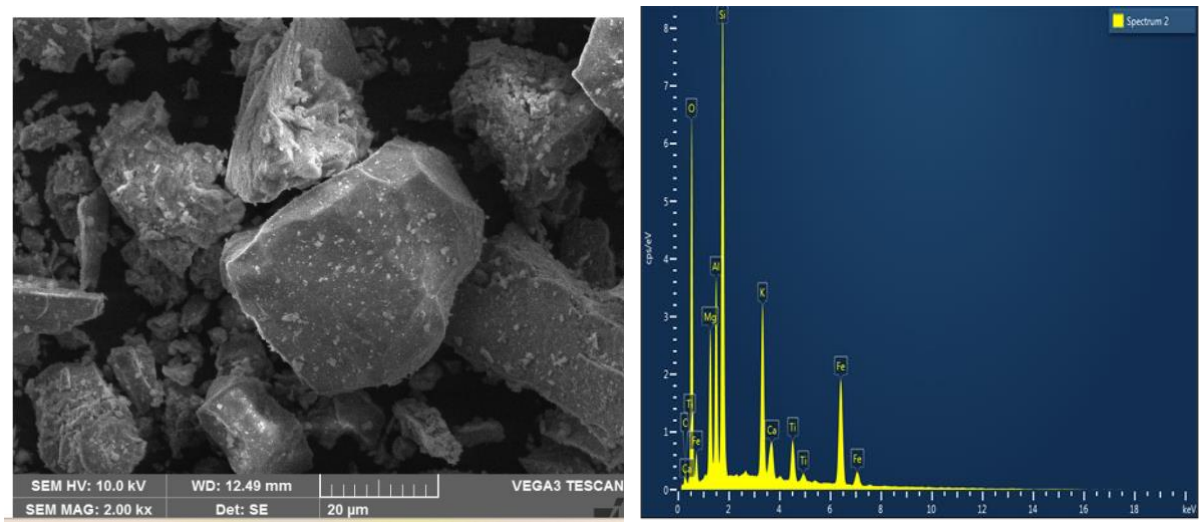

Fig. 17. SEM and EDX image of A12 concrete (20% GGBS & 10% SCBA as binder)

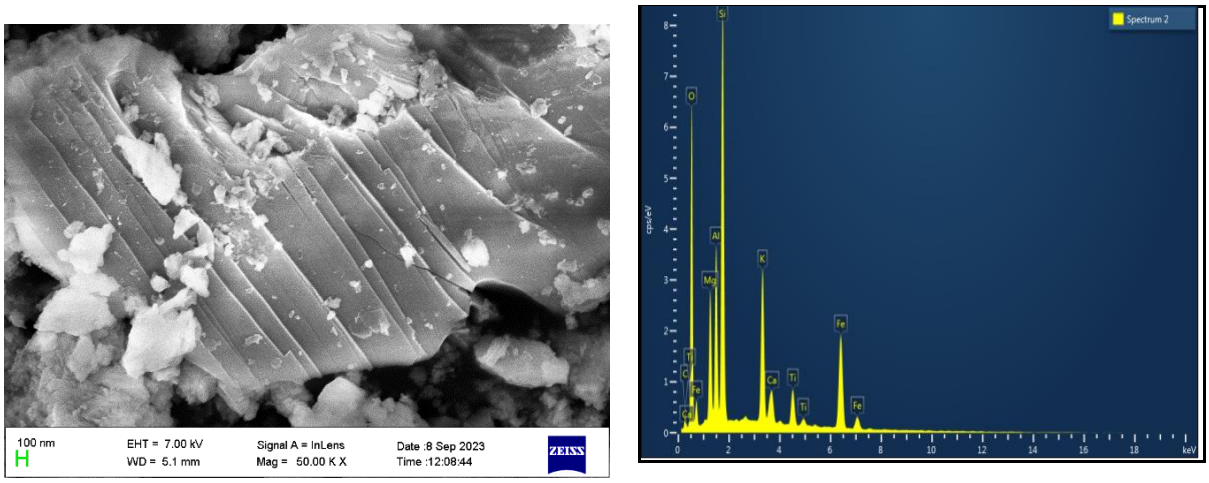

Fig. 18. SEM and EDX image of A22 concrete (20% GGBS and 10% SCBA as binder+5 % SCBA as FA)

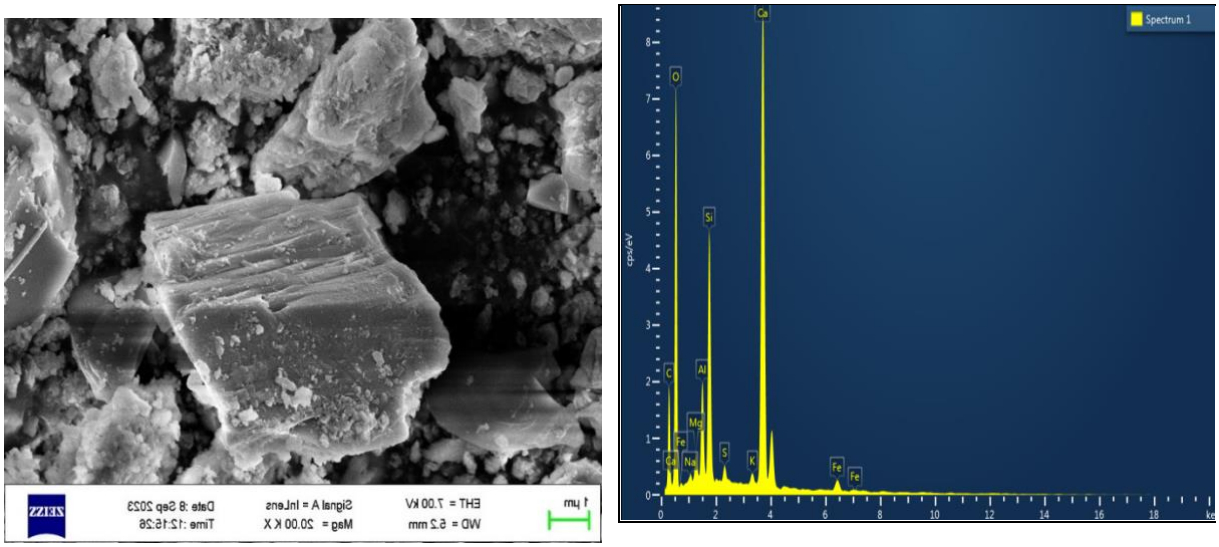

Fig. 19. SEM and EDX image of A32 concrete (20% GGBS and 15% SCBA as binder)

The SEM and EDX images for the control and a few mixes are shown in Fig.16 to 19. The SEM images of the samples with binder replacement show clear gel formation, which leads to strength from the C-S-H bonds formed during hydration. Upon 28 days of curing, the concrete shows a compact and well-developed C–S–H structure with minimal porosity, reflecting significant pozzolanic activity. According to the investigation, secondary pozzolanic reactions that enhance and improve the microstructure are caused by interactions between SCBA and GGBS particles and portlandite created during cement hydration. When SCBA and GGBS were added, the microstructure became more compact, most likely because these samples had higher SiO_2 levels than previous combinations.

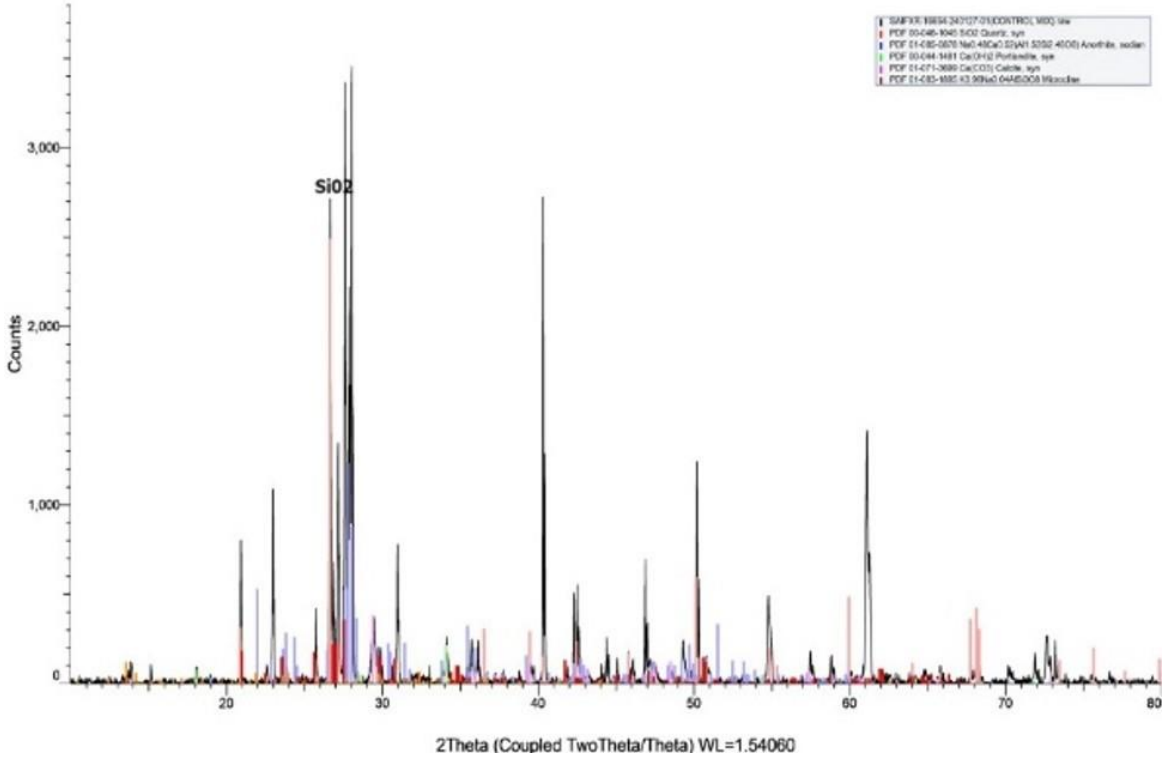

Fig. 20. XRD image of control concrete

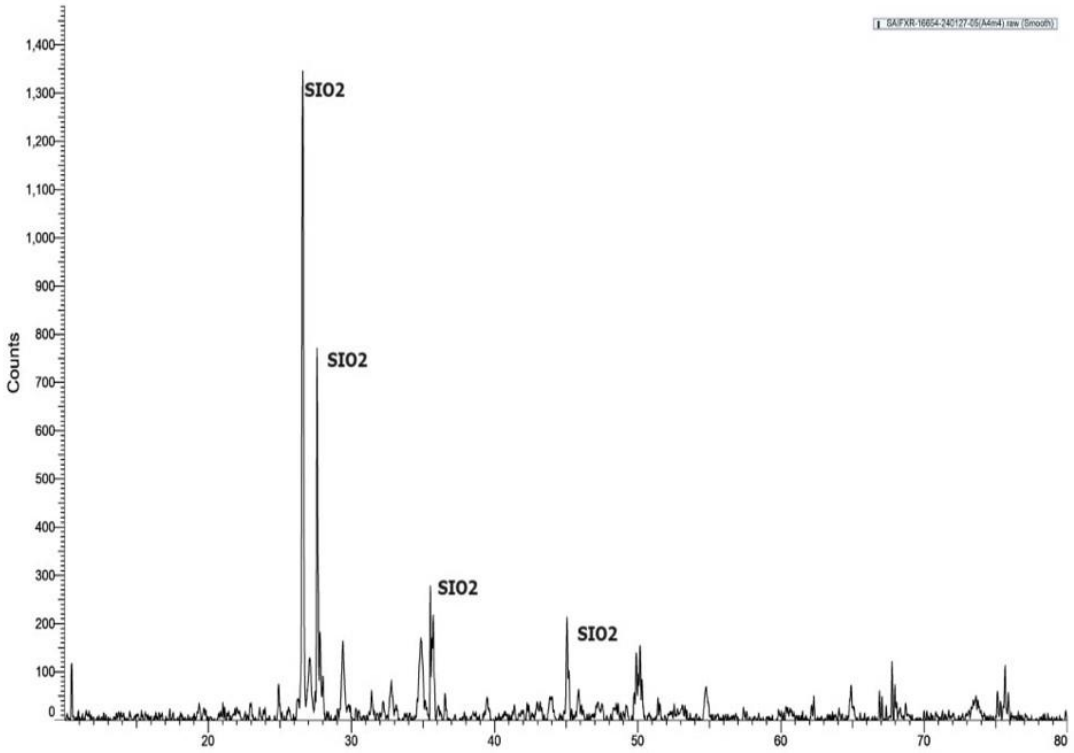

Fig. 21. XRD image of A12 concrete (20% GGBS and 10% SCBA as binder)

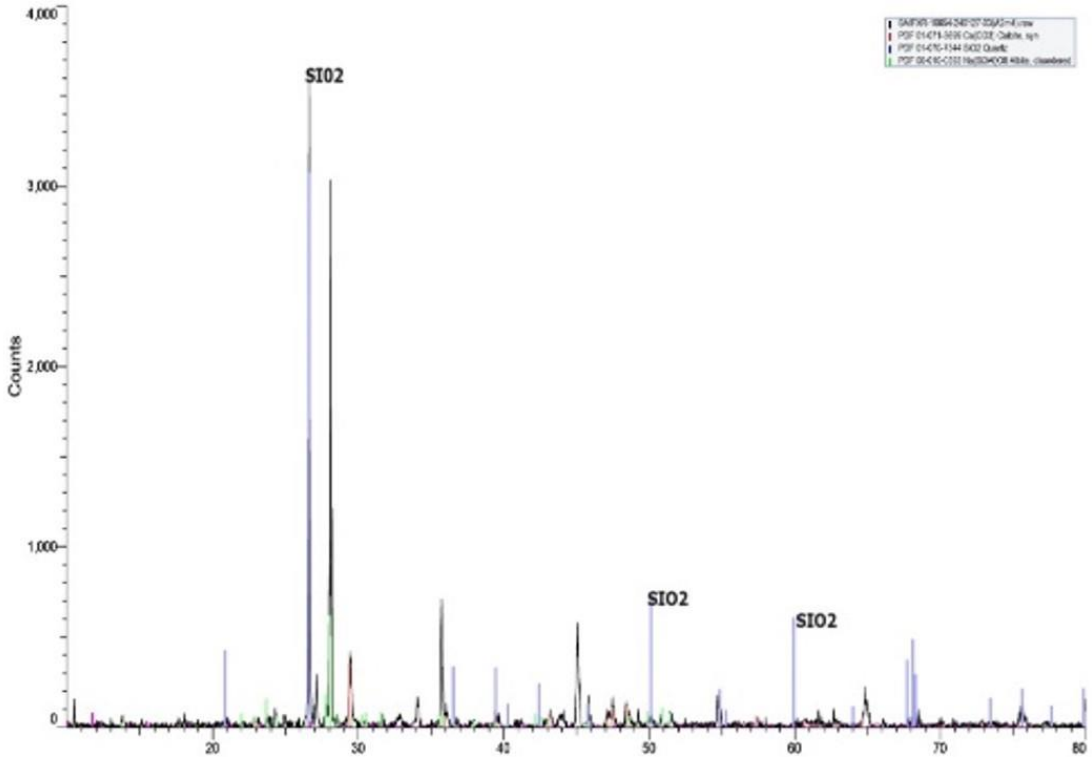

Fig. 22. XRD image of A22 concrete (20% GGBS and 10% SCBA as binder+5 % SCBA as FA)

The XRD results for the control mix and the mixes whose compressive strengths are quite similar to the control are shown in Figs. 20–23. Following the compressive strength test, some of the structure was taken out of the cube. With a wavelength (WL) of 1.54060 Å, a Cu Kα radiation source was used to powder this matrix and perform XRD analysis. The diffraction pattern was captured between 10° and 80° across a 2θ range. Near 26.6°, the strongest peak is associated with quartz (SiO_2). This phase is a major constituent in concrete aggregates and contributes to the bulk mineral

content. The X-ray diffraction (XRD) patterns reveal prominent peaks corresponding to quartz (SiO_2), portlandite ($Ca(OH)_2$), and calcite ($CaCO_3$), along with minor aluminosilicate phases such as anorthite and microcline. The enhanced microstructure and pozzolanic activity resulting from the addition of supplementary cementitious materials are evident in the increased intensity of hydration products, particularly portlandite. The presence of these stable crystalline phases supports the observed improvements in mechanical strength and durability, underscoring the effectiveness of SCBA and GGBS in enhancing the concrete matrix and contributing to more sustainable construction practices.

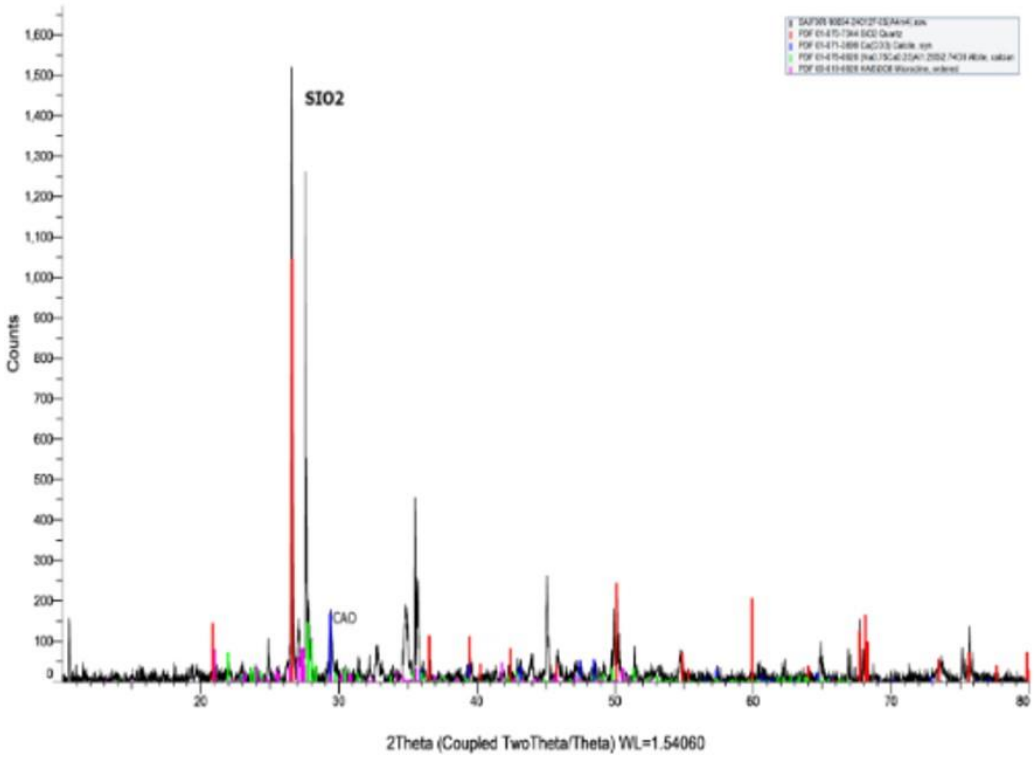

Fig. 23. XRD image of A32 concrete (20% GGBS and 15% SCBA as binder)

4. Sustainability Assessment

Table 7 shows the gross carbon di oxide emission at various replacement level of concrete developed by GGBS and SCBA. From mix design 410 kg of cement is calculated for 1m^3 control mix. GGBS and SCBA at a percentage of 0- 40 and 10 to 15 were taken for the study. Emission factors used were 0.9 kg CO_2 per kg of OPC, 0.14 kg CO_2 per kg of GGBS, and 0.11 kg CO_2 per kg of SCBA. [40,41,42]. The replacement of cement with combined GGBS and SCBA significantly reduced CO_2 emissions, with gross CO_2 savings increasing proportionally with higher SCM content. The maximum CO_2 saving of 173.23 kg/m^3 was observed for the mix containing 40% GGBS + 15% SCBA, while the minimum saving of 63.55 kg/m^3 occurred at 10% GGBS + 10% SCBA. Concrete mixes with 20% GGBS combined with 10% SCBA and 20% GGBS combined with 15% SCBA demonstrated strengths comparable to the control mix, while achieving significant CO2 emission reductions of 94.71 kg/m^3 and 110.95 kg/m^3, respectively. Overall results shows that partial replacement of cement with SCBA and GGBS reduce CO_2 emission while maintaining comparable strength.

Several studies showed that fly ash and silica fume reduce the CO_2 emissions of concrete by partially replacing Portland cement, though their performance varies with processing energy and transportation distance. Fly ash offers moderate emission reduction benefits as an industrial by-product, whereas silica fume shows relatively higher emission intensity due to its energy-intensive production process [43]. When combined with low emission SCBA, the GGBS–SCBA blend provides a higher sustainability advantage while maintaining satisfactory mechanical performance.

Table 7. Gross and Net CO_2 Emission Savings at Various GGBS+SCBA Replacement

Mix	Mass of cement replaced by SCM (kg/m^3)	Mass of GGBS (kg/m^3)	Mass of SCBA (kg/m^3)	Reduction in Carbon di oxide emission =Mass of cement replaced x 0.9(kg CO_2/m^3)	CO2 emission in SCM (GGBS×0.14 + SCBA×0.11) kg CO_2/m^3	Gross CO_2 reduction (kg CO_2/m^3)
10% GGBS + 10% SCBA	82	41	41	73.8	10.25	63.55
20% GGBS + 10% SCBA	123	82	41	110.7	15.99	94.71
30% GGBS + 10% SCBA	164	123	41	147.6	21.73	125.87
40% GGBS + 10% SCBA	205	164	41	184.5	27.47	157.03
10% GGBS + 15% SCBA	102.5	41	61.5	92.25	12.505	79.745
20% GGBS + 15% SCBA	143.5	82	61.5	129.15	18.245	110.905
30% GGBS + 15% SCBA	184.5	123	61.5	166.05	23.985	142.065
40% GGBS + 15% SCBA	225.5	164	61.5	202.95	29.725	173.225

5. Conclusion

Concrete developed by blending GGBS and SCBA shows good workability with slump values between 75 mm to 120mm. The increase in GGBS content raised the slump value because of its smooth and fine structure. On the other hand, mixes containing SCBA had lower slump values. It is due to high porosity and large surface area that causes water demand and reduced flowability. Mechanical and microstructural studies found that replacing cement up to 35 % with GGBS and SCBA resulted in concrete with a dense structure and strength comparable to that of the reference mix. Compressive strength of mixes with 20% GGBS and 10–15% SCBA had strengths comparable to the control mix. These mixes show a positive effect of their pozzolanic reactions.

The higher the level of GGBS replacement, the greater the reduction in strength. Split tensile strength shows a comparable pattern to compressive strength. For both cases the optimum binder replacement is 30 percent. Flexural strength also decreased slightly as replacement levels increased. The fine particle size and high silica content aided the formation of C–S–H gel. The presence of approximately 38% lime in GGBS improved the workability of the concrete, while the higher silica content of about 32% in GGBS and 62% in SCBA contributed significantly to the strength development in the ternary blend concrete.

A mathematical model was developed with the help of experimental data to predict compressive strength and flexural strength for different proportions of GGBS and SCBA. Validation against experimental data of compressive strength and split tensile strength shows errors below 5%, indicating that the model is reliable.

Combined replacements of 10–40% GGBS and 10–15% SCBA led to gross savings of 64–173 kg /m^3 of CO_2. The optimum mixes with 20 to 35% binder replacement gives a carbon di oxide savings of 95 to 110 kg/m^3. The results of this study indicate that the addition of GGBS and SCBA can be effectively adopted in the construction industry to reduce cement consumption for sustainable concrete. Future investigations must address the long-term durability characteristics of GGBS–SCBA blended concrete.

Reference

[1] Alvarenga KP, Cordeiro GC. Evaluating sugarcane bagasse fly ash as a sustainable cement replacement for enhanced performance. Clean Eng Technol. 2024;20:100751. https://doi.org/10.1016/j.clet.2024.100751

[2] Zareei SA, Ameri F, Bahrami N. Microstructure, strength, and durability of eco-friendly concretes containing sugarcane bagasse ash. Constr Build Mater. 2018;184:258–268. https://doi.org/10.1016/j.conbuildmat.2018.06.153

[3] Athira G, Bahurudeen A, Sahu PK, Santhanam M, Nanthagopalan P, Lalu S. Effective utilization of sugar industry waste in Indian construction sector: A geospatial approach. J Mater Cycles Waste Manag. 2020;22:724–736. https://doi.org/10.1007/s10163-019-00963-w

[4] Orozco C, Babel S, Tangtermsirikul S, Sugiyama T. Comparison of environmental impacts of fly ash and slag as cement replacement materials for mass concrete and the impact of transportation. Sustain Mater Technol. 2024;39:e00796. https://doi.org/10.1016/j.susmat.2023.e00796

[5] Sales A, Almeida FCR, et al. Joint use of construction waste (CW) and sugarcane bagasse ash sand (SBAS) in concrete. Constr Build Mater. 2016;113:317–323. https://doi.org/10.1016/j.conbuildmat.2016.03.062

[6] García-Troncoso N, Hidalgo-Astudillo S, Tello-Ayala K, Gutiérrez-González S, Cabrera-Covarrubias F. Preparation and performance of sugarcane bagasse ash pavement repair mortars. Case Stud Constr Mater. 2023;19:e02563. https://doi.org/10.1016/j.cscm.2023.e02563

[7] Karikatti V, Chitawadagi MV, Devarangadi M. Influence of bagasse ash powder and marble powder on strength and microstructure characteristics of alkali-activated slag concrete cured at room temperature for rigid pavement application. Clean Mater. 2023;9:100200. https://doi.org/10.1016/j.clema.2023.100200

[8] Kirthiga R, Elavenil S. Potential utilization of sugarcane bagasse ash in cementitious composites for developing inorganic binder. Ain Shams Eng J. 2023;14:102560. https://doi.org/10.1016/j.asej.2023.102560

[9] Chusilp N, Jaturapitakkul C, Kiattikomol K. Utilization of bagasse ash as a pozzolanic material in concrete. Constr Build Mater. 2009;23(11):3352–3358. https://doi.org/10.1016/j.conbuildmat.2009.06.030

[10] Bahurudeen A, Santhanam M. Influence of different processing methods on the pozzolanic performance of sugarcane bagasse ash. Cem Concr Compos. 2015;56:32–45. https://doi.org/10.1016/j.cemconcomp.2014.11.002

[11] Ramakrishnan K, Ganesh V, Vignesh G, Vignesh M, Shriram V, Suryaprakash R. Mechanical and durability properties of concrete with partial replacement of fine aggregate by sugarcane bagasse ash (SCBA). Mater Today Proc. 2021;42:1070–1076. https://doi.org/10.1016/j.matpr.2020.12.172

[12] Arenas-Piedrahita JC, Montes-García P, Mendoza-Rangel JM, Calvo HL, Valdez-Tamez PL, Martínez-Reyes J. Mechanical and durability properties of mortars prepared with untreated sugarcane bagasse ash and untreated fly ash. Constr Build Mater. 2016;105:69–81. https://doi.org/10.1016/j.conbuildmat.2015.12.047

[13] Kumar VP, Gunasekaran K, Shyamala T. Characterization study on coconut shell concrete with partial replacement of cement by GGBS. J Build Eng. 2019;26:100830. https://doi.org/10.1016/j.jobe.2019.100830

[14] Phul AA, Memon MJ, Shah SNR, Sandhu AR. GGBS and fly ash effects on compressive strength by partial replacement of cement concrete. Civil Eng J. 2019;5(4):913–921. http://dx.doi.org/10.28991/cej-2019-03091299

[15] Khalil MJ, Aslam M, Ahmad S. Utilization of sugarcane bagasse ash as cement replacement for the production of sustainable concrete–A review. Constr Build Mater. 2021;270:121371. https://doi.org/10.1016/j.conbuildmat.2020.121371

[16] Wu N, Ji T, Huang P, Fu T, Zheng X, Xu Q. Use of sugar cane bagasse ash in ultra-high performance concrete (UHPC) as cement replacement. Constr Build Mater. 2022;317:125881. https://doi.org/10.1016/j.conbuildmat.2021.125881

[17] Liu Z, Takasu K, Koyamada H, Suyama H. A study on engineering properties and environmental impact of sustainable concrete with fly ash or GGBS. Constr Build Mater. 2022;316:125776. https://doi.org/10.1016/j.conbuildmat.2021.125776

[18] Venkat GN, Chandramouli K, NagendraBabu V. Comparative study on mechanical properties and quality of concrete by part replacement of cement with silica fume, metakaolin and GGBS by using M–Sand as fine aggregate. Mater Today Proc. 2021;43:1874–1878. https://doi.org/10.1016/j.matpr.2020.10.819

[19] Krishna BR, Kumar KH, Kumar TM, Likitha I. Properties of GGBS concrete under various curing conditions. Int J Civ Eng Technol. 2020;8(4):123–130. https://doi.org/10.30534/ijeter/2020/72842020

[20] Abdalla TA, Koteng DO, Shitote SM, Matallah M. Mechanical and durability properties of concrete incorporating silica fume and high volume sugarcane bagasse ash. Results Eng. 2022;16:101635. https://doi.org/10.1016/j.rineng.2022.100666

[21] Sobuz MHR, Datta SD, Jabin JA, Aditto FS, Hasan NMS, Hasan M, Zaman AAU. Assessing the influence of sugarcane bagasse ash for the production of eco-friendly concrete: Experimental and machine learning approaches. Case Stud Constr Mater. 2024;20:e02839. https://doi.org/10.1016/j.cscm.2023.e02839
[22] Topçu İB. Physical and mechanical properties of concretes produced with waste concrete. Cem Concr Res. 1997;27(12):1817–1823. https://doi.org/10.1016/S0008-8846(97)00190-7
[23] Bureau of Indian Standards. IS 1199:2018 – Methods of sampling and analysis of concrete. New Delhi: Bureau of Indian Standards; 2018.
[24] Bureau of Indian Standards. IS 516:2021 – Methods of tests for strength of concrete (Section 1, Part 1). New Delhi: Bureau of Indian Standards; 2021.
[25] Yahyaee T, Elize HS. A comprehensive study on mechanical properties, durability, and environmental impact of fiber-reinforced concrete incorporating ground granulated blast furnace slag. Case Stud Constr Mater. 2024;20:e03190. https://doi.org/10.1016/j.cscm.2024.e03190
[26] Nasir S, Elhameed HAA, Fadhil NM, Hashem AM. Effects of sugarcane bagasse ash on the properties of concrete. Proc Inst Civ Eng Eng Sustain. 2018;171(3):123–132. https://doi.org/10.1680/jensu.15.00014
[27] Bheel N, Khoso S, Baloch M, Benjeddou O, Alwetaishi M. Use of waste recycling coal bottom ash and sugarcane bagasse ash as cement and sand replacement material to produce sustainable concrete. Environ Sci Pollut Res. 2022. https://doi.org/10.1007/s11356-022-19478-3
[28] García-Troncoso N, Hidalgo-Astudillo S, Tello-Ayala K, et al. Preparation and performance of sugarcane bagasse ash pavement repair mortars. Case Stud Constr Mater. 2023;19:e02563. https://doi.org/10.1016/j.cscm.2023.e02563
[29] Rukzon S, Chindaprasirt P. Utilization of bagasse ash in high-strength concrete. Mater Des. 2012;34:45-50. https://doi.org/10.1016/j.matdes.2011.07.045
[30] Wang L, Zheng D, Zhang S, Cui H, Li D. Effect of nano-SiO_2 on the hydration and microstructure of Portland cement. Nanomaterials. 2016;6(12):241. https://doi.org/10.3390/nano6120241
[31] Katare VD, Madurwar MV. Experimental characterization of sugarcane biomass ash–A review. Constr Build Mater. 2017;152:1–15. https://doi.org/10.1016/j.conbuildmat.2017.06.142
[32] Ganesan K, Rajagopal K, Thangavel K. Evaluation of bagasse ash as supplementary cementitious material. Cem Concr Compos. 2007;29(6):515–524. https://doi.org/10.1016/j.cemconcomp.2007.03.001
[33] Srinivasan R, Sathiya K. Experimental study on bagasse ash in concrete. Int J Serv Learn Eng. 2010;5(2):60–66. https://doi.org/10.24908/ijsle.v5i2.2992
[34] Sathiparan N, Dassanayake DHHP, Subramaniam DN. Utilization of supplementary cementitious materials in pervious concrete: A review. Int J Environ Sci Technol. 2024;21(6):5883–5918. https://doi.org/10.1007/s13762-023-05440-4
[35] Ahmad J, Martínez-García R, Szelag M, de-Prado-Gil J, Marzouki R, Alqurashi M, Hussein EE. Effects of steel fibers (Sf) and ground granulated blast furnace slag (ggbs) on recycled aggregate concrete. Materials. 2021;14(24):7497. https://doi.org/10.3390/ma14247497
[36] Xu Q, Ji T, Gao SJ, Yang Z, Wu N. Characteristics and applications of sugar cane bagasse ash waste in cementitious materials. Materials. 2018;12(1). https://doi.org/10.3390/ma12010039
[37] Bahurudeen A, Wani K, Basit MA, Santhanam M. Assesment of pozzolanic performance of sugarcane bagasse ash. J Mater Civ Eng. 2016;28(2):04015095. https://doi.org/10.1061/(ASCE)MT.1943-5533.0001361
[38] Gupta CK, Sachan AK, Kumar R. Examination of microstructure of sugar cane bagasse ash and sugar cane bagasse ash blended cement mortar. Sugar Tech. 2021;23(3):651-660. https://doi.org/10.1007/s12355-020-00934-8
[39] Zhang P, Liao W, Kumar A, Zhang Q, Ma H. Characterization of sugarcane bagasse ash as a potential supplementary cementitious material: Comparison with coal combustion fly ash. J Clean Prod. 2020;277:123834. https://doi.org/10.1016/j.jclepro.2020.123834
[40] Ullah MF, Tang H, Ullah A, Toth Z, Ahmad M, Alzlfawi A. Mechanical and environmental performance of sugarcane Bagasse Ash from Khyber Pakhtunkhwa in sustainable concrete. Sci Rep. 2025;15(1):24571. https://doi.org/10.1038/s41598-025-10383-6
[41] Khaiyum MZ, Sarker S, Kabir G. Evaluation of carbon emission factors in the cement industry: An emerging economy context. Sustainability. 2023;15(21):15407. https://doi.org/10.3390/su152115407
[42] Ige OE, Von Kallon DV, Desai D. Carbon emissions mitigation methods for cement industry using a systems dynamics model. Clean Technol Environ Policy. 2024;26(3):579-597. https://doi.org/10.1007/s10098-023-02683-0
[43] Singh GB, Prasad VD. Environmental impact of concrete containing high volume fly ash and ground granulated blast furnace slag. J Clean Prod. 2024;448:141729. https://doi.org/10.1016/j.jclepro.2024.141729